

Determination of Clearance to the Stop based on Performance Criteria of a Seismically Isolated Nuclear Power Plant

Minkyu Kim¹, Gyeonghee An²

¹ Principal Researcher, Korea Atomic Energy Research Institute, Daejeon, Korea

² Senior Researcher, Korea Atomic Energy Research Institute, Daejeon, Korea (akh425@kaeri.re.kr)

ABSTRACT

The clearance to the stop (CS), which refers to the horizontal distance between the superstructure of isolated NPP and the physical stop, is an important matter affecting the risk assessment of isolated NPPs. The objective of this paper is to evaluate the CS requirements based on the performance criteria. To satisfy these criteria, the CS has to be greater than the 90th percentile displacement of the structure under beyond design basis earthquake (BDBE) ground motions, and the isolation system needs to be designed to have 90% confidence or higher for the CS. The 90th percentile displacement under BDBE ground motions is analytically determined. The numerical model of a lead rubber bearing (LRB) was suggested based on the full-scale test results for reasonable seismic response. Capacity of isolator is experimentally determined. Failure probability can be calculated by maximum likelihood estimation using experimental results. The 10th percentile from the failure probability of isolator can be the upper bound of the CS to satisfy the performance criteria. Limitations of this study include insufficient numbers of experiments as well as analysis results that are dependent on the particular models, ground motions, and criteria selected. Further research is necessary to suggest more reasonable ranges of CS.

INTRODUCTION

In this research, an NPP model was built based on the APR1400 (Advanced Power Reactor 1400 MW) from the Republic of Korea with lead rubber bearings (LRBs) used for the isolation system. The structural model was initially developed by KEPCO E and C (Korea Electric Power Corporation Engineering and Construction Company), which is in charge of the APR1400 design, and later converted to OpenSees in collaboration with the University of California, Berkeley [Schellenberg et al., 2015]. The model was then modified for the current study as well as related research to include moat walls [Sarebanha et al., 2018] and advanced bearing models to capture the nonlinear characteristics of the LRBs [Mosqueda et al., 2019]. The bearing models focus on capturing experimental results at large shear strain to better reflect strong ground motions. In the present work, the response of an isolated NPP including the displacement of the isolation system and floor response spectra (FRS) is investigated using the analytical model combining both structural and bearing models.

The key objective of this paper is to examine the performance criteria of seismically isolated NPPs, particularly the clearance to the stop (CS), as suggested by NUREG [USNRC, 2019] and ASCE [2017]. A physical stop is necessary for seismically isolated NPPs to ensure the mean annual frequency of failure of the isolation system is very small. The CS, which refers to the horizontal distance between the superstructure of isolated NPP and the physical stop, is an important matter affecting the risk assessment of isolated NPPs, but few studies have evaluated CS. Kumar and Whittaker [2015] calculated CS considering responses from various ground motions but the capacity of the isolation system was not considered. In the current paper, both numerical simulations and the experimental results from the bearing

test program are considered in evaluating the range of CS. The lower and upper bounds of CS are suggested from the analytical displacement response and the experimental capacity of the isolators, respectively.

PERFORMANCE CRITERIA

The performance criteria for seismically isolated nuclear structures has been suggested in standards such as ASCE 4–16 [2017] and NUREG/CR-7253 [USNRC, 2019]. According to the standards, seismically isolated NPPs should allow for sufficient displacement of the isolation layer to reduce the acceleration induced by ground motions, while the failure probabilities of the superstructure, isolation systems, and umbilical lines remain at low levels, as specified below.

NUREG/CR-7253 gives performance and design recommendations for seismically isolated NPPs at two levels of ground motion: GMRS+ and BDBE GMRS. The first, GMRS+, covers RG1.208 GMRS and the minimum foundation input motion, while the second, BDBE GMRS, covers the UHRS (uniform hazard response spectrum) at a mean annual frequency of exceedance of 1×10^{-5} and 167% of GMRS+. The criteria under BDBE GMRS loading are normally critical. Isolation systems need to have 90% confidence of surviving without loss of gravity-load capacity, and the superstructure needs to have less than a 10% probability of contacting with a hard stop (moat wall) under BDBE GMRS loading. To satisfy these criteria, the CS has to be greater than the 90th percentile displacement of the structure under BDBE GMRS loading, and the isolation system and umbilical lines need to be designed to have 90% confidence or higher for the CS. The capacity of the interfacing components such as the umbilical lines is assumed in this work, and thus the failure of the umbilical lines is not considered at present.

CAPACITY OF THE ISOLATION SYSTEM

Experimental Setup

To obtain more data on the capacity of the LRBs, additional experiments were conducted on bearings smaller in size than those presented earlier for the model development. The dimensions of the LRB specimens are shown in Figure 1 [Kim et al., 2019]. The diameters of the LRB and lead core were 550 mm and 120 mm, respectively, and the total rubber thickness was 112 mm. Fifteen specimens, as listed in Table 1, were tested until failure. It should be noted that these specimens had experienced horizontal loading prior to the failed test and could have been slightly damaged; the LRBs were therefore classified as low damage (LD), moderate damage (MD), and high damage (HD) for previously experienced shear strain levels of 100%, 300%, and 400%, respectively. The fourth column in Table 1 lists the experimental variable P/Pd, which is the ratio of the axial load to the design axial load, ranging from 0 to 6. Each test was performed by horizontal displacement control loading under these axial loading conditions.

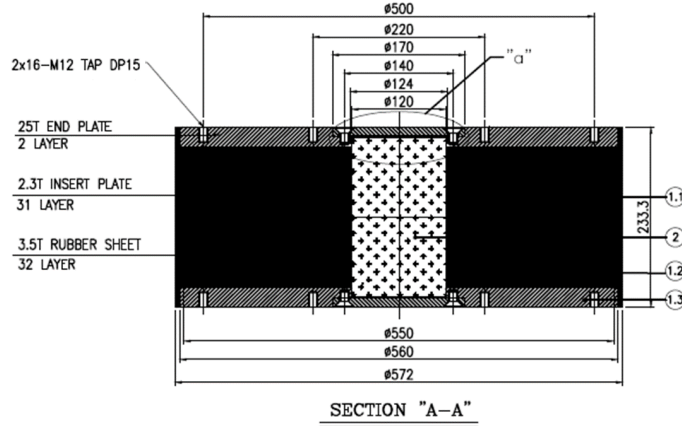


Figure 1. LRB specimen dimensions.

Table 1. Specimens for the ultimate property test.

Test Sequence	Specimen	Tag	P/P _d	Vert. Load (kN)	Buckling Load (kN)	Failure Load (kN)	Failure Disp. (mm)	Failure Disp. (%)
#1	UCSD300%(1)	MD-P1.0	1.0	2942		683	457	408
#2	UCSD300%(5)	MD-P1.0	1.0	2942		762	462	412
#3	UCSD Non(1)	LD-P1.0	1.0	2942		460	389	348
#4	UCSD400%(1)	HD-P1.0	1.0	2942	236	583	478	427
#5	SGS1.0Pd	MD-P1.0	1.0	2942		777	470	419
#6	UCSD Non(2)	LD-P6.0	6.0	17,649		245	67	60
#7	UCSD300%(3)	MD-P2.0	2.0	5883	232	766	480	429
#8	UCSD300%(7)	MD-P3.0	3.0	8825	311	666	476	425
#9	SGS1.5Pd	MD-P1.5	1.5	4412	287	761	467	417
#10	UCSD300%(4)	MD-P2.5	2.5	7354	214	614	457	408
#11	UCSD300%(8)	MD-P4.0	4.0	11,766	180	594	460	410
#12	SGS2.0Pd	MD-P5.0	5.0	14,708	126	666	483	431
#13	UCSD300%(2)	MD-P0.0	0.0	500		782	463	413
#14	UCSD400%(2)	HD-P0.0	0.0	500		597	477	426
#15	UCSD300%(6)	MD-P0.5	0.5	1471		763	469	419

Ultimate Property Diagram

The failure criteria of the LRBs can be represented by an ultimate property diagram (UPD). The vertical load on an LRB affects its failure mode and shear failure capacity; the UPD shows this relationship, namely between the axial load and the shear load or strain of the limit state. In this research, UPDs were predicted experimentally because of difficulties in numerical analysis.

Figure 2a and b show UPDs based on the failure load and failure strain, respectively, from the test results in Table 1. As can be seen in the figure, the failure strains of the specimens are rather consistent at about 420%, compared to the failure loads. Therefore, within a certain level of vertical load, the shear strain can be a failure criteria parameter.

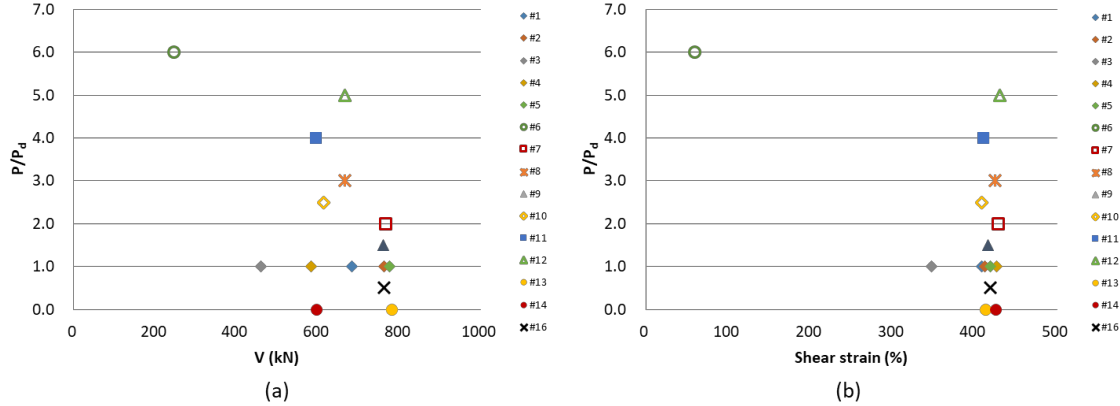


Figure 16. Ultimate property diagram in (a) shear force and (b) shear strain.

Models for Numerical Analysis

Structural Model of the APR1400

The structural model of the APR1400 including a seismic isolation system consisting of 486 bearings was initially developed in SAP2000 by KEPCO E and C. KEPCO, which is in charge of designing NPPs in Korea, developed a simplified Archetype Nuclear Test (ANT) stick model, as shown in Figure 3 [Mosqueda and Sarebanha, 2018]. The superstructure is modeled as beam–stick elements with lumped masses and the base mat is modeled using three dimensional solid elements. The reactor containment building (RCB) and the auxiliary building (AB) are located at the center of the model. The isolators are attached at the bottom of the base mat. The total weight of the nuclear island including base mat, reactor, RCB, and AB is 4732 MN. This SAP2000 model was then converted to an OpenSees format for hybrid simulations and parametric analysis [Schellenberg et al., 2015].

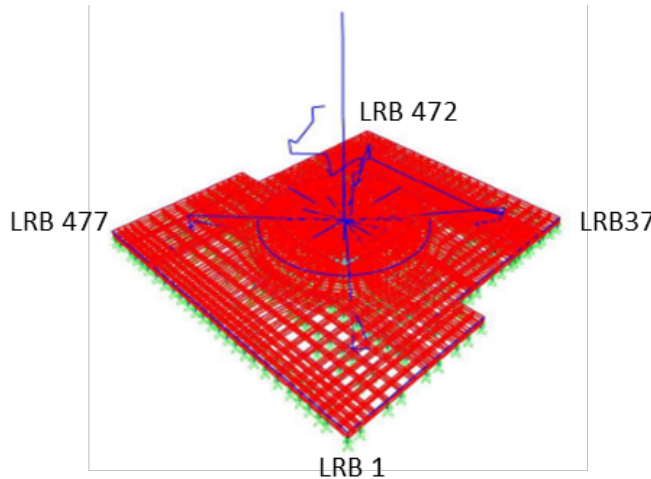


Figure 3. ANT model.

Isolator Model

KAERI conducted full-scale tests of LRBs designed for NPPs in 2014. As shown in the schematic in Figure 4, the diameters of the LRB and lead core were 1500 mm and 320 mm, respectively, with 32 layers of 7 mm thick rubber stacked to give a total rubber height of 224 mm. Two LRBs were tested,

where each specimen experienced various motions including sine wave motion, elliptical trace sinusoidal motion, and earthquake response motion. Shear strain up to 500% at three frequencies (0.01 Hz, 0.2 Hz, and 0.5 Hz) was tested at the design axial load, 22,000 kN. Detailed explanations of the experiments can be found in previous reports [Kim, M. et al., 2019, Kim, J. et al., 2019]; Figure 5 presents an example of experimental results obtained from the tests.

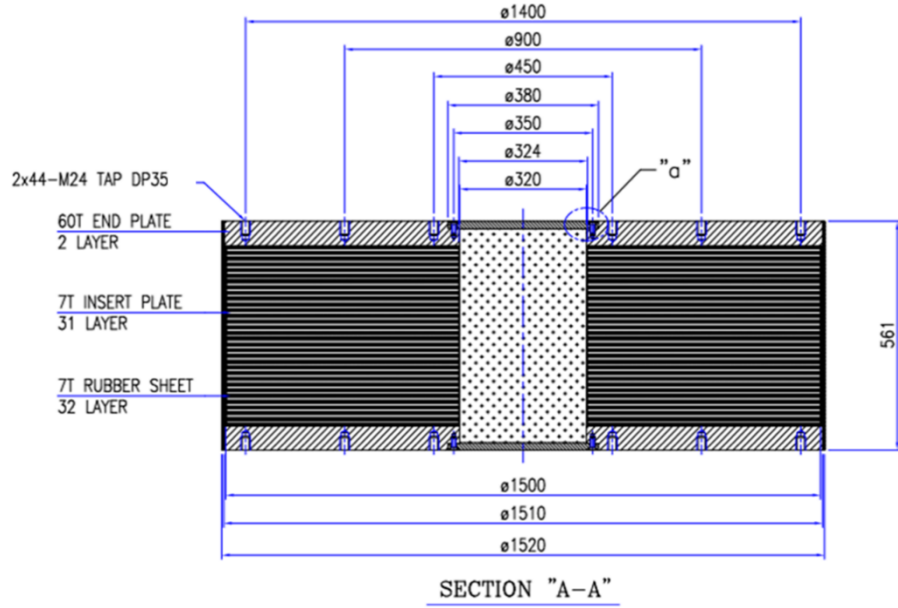


Figure 4. Dimensions of the test bearings (unit: mm).

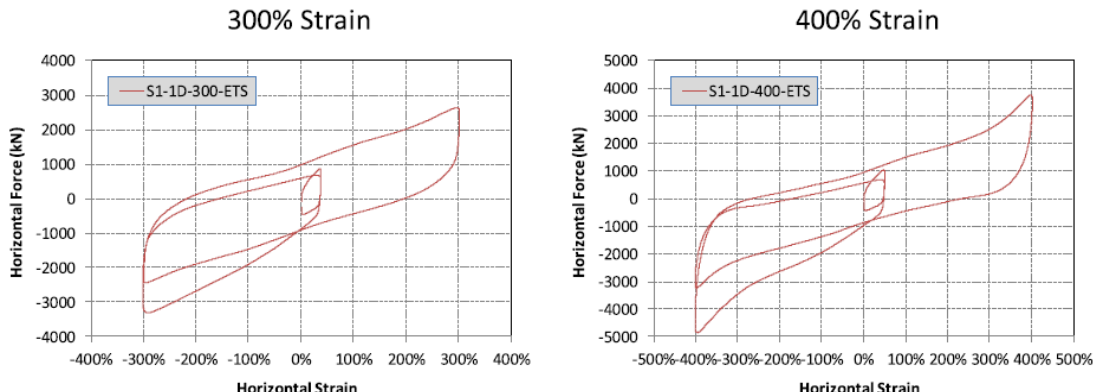


Figure 5. Strain-force curves in the unidirectional sinusoidal test [13].

A parallel numerical model of an isolator representing an LRB was suggested by Mosqueda, Marquez, and Hughes [2019]. The characteristic behaviors of the LRBs, such as a reduction in strength due to the heat of the lead and hardening at large strain, as shown in Figure 5, are modeled using three elements: an LRX element, a Bouc–Wen (hardening) element, and an HDR element, which are all separately available in OpenSees, as shown in Figure 6.

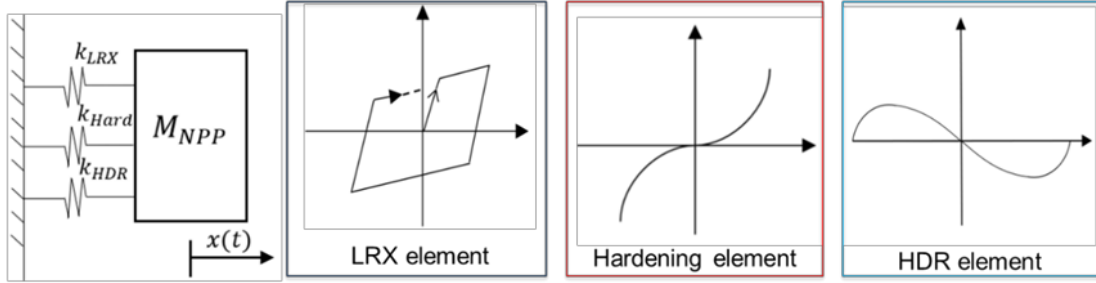


Figure 6. Parallel system of the bearing model.

Ground Motions

The Pacific Earthquake Engineering Research Center (PEER) published a technical report [Schellenberg et al., 2014] as the outcome of a research project conducted in tandem with KEPCO. In this project, a set of 20 ground motions were selected from the PEER NGA-West1 database, such that they match the mean and dispersion of a target response spectrum. Using RSPMatch, each of the selected dispersion-appropriate records was individually matched to a single target spectrum corresponding to 5% damping.

Response of an Isolated Nuclear Power Plant

Displacement of the Isolation System and Upper Structures

Figure 6 shows the force-displacement relation of an LRB (LRB #1) subjected to the same ground motion but at various PGA levels. This bearing, as depicted in Figure 3, is located at the corner of the base mat. According to Figure 7, the bearing model shows increased nonlinearity as the ground motion strengthens, similar to experimental observations, and thus it can be concluded that the bearing model is suitable for beyond design basis applications.

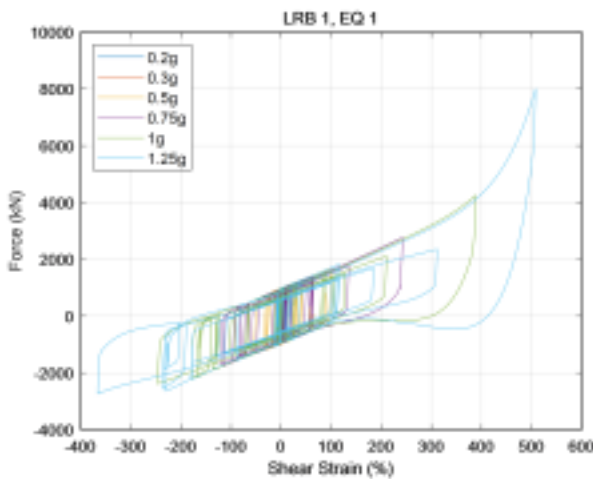


Figure 7. Hysteresis of LRB #1.3.2. Floor Response Spectra of an Isolated NPP.

The floor response spectra (FRS) is another essential aspect in the analysis of the seismic fragility of equipment as well as risk assessment. Figure 8 shows a comparison of the FRS from both base-isolated and non-isolated RCBs. The isolation system reduces the overall responses of the structure, with the

isolated RCB only slightly exceeding the non-isolated RCB in the region near the natural frequency of the isolation system.

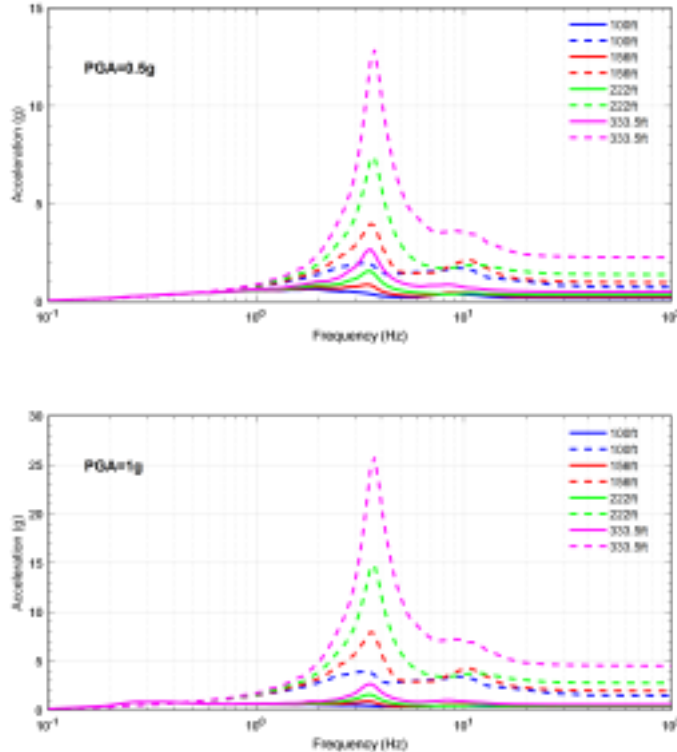


Figure 8. Comparison of FRS at different PGA from isolated (solid lines) and non-isolated (dashed lines) RCBs.

If there exists a stop (moat wall) in accordance with the evaluated CS, the FRS of the base-isolated RCB can be amplified due to a collision between the wall and the base mat, especially for ground motions exceeding BDBE ground motion response spectra (GMRS). Therefore, further research for the modeling of the moat wall, backfill soil, and impact is necessary to evaluate FRS considering moat wall impact at strong ground motions.

DETERMINATION OF CLEARANCE TO HARD STOP

Lower Bound of CS from Displacement Response

The RG1.60 design spectrum with $\text{PGA} = 0.5\text{g}$ can be regarded as the GMRS in the present work because a specific target site was not designated, and therefore the 20 ground motions detailed in Section 2.3 were selected for the analysis. An amplification factor AR was calculated to be about 2 because the ratio of the peak ground acceleration at an annual frequency of exceedance of 10^{-4} and 10^{-5} is about 2 based on a related hazard analysis in Korea [Kim. et al., 2012]. Therefore, the BDBE GMRS is assumed as the RG1.60 design spectrum with $\text{PGA} = 1.0 \text{ g}$.

Figure 9 shows a histogram of the maximum displacements of the AB at ground level (height = 100 ft) subjected to 20 ground motions for BDBE GMRS loading ($\text{PGA} = 1.0 \text{ g}$).

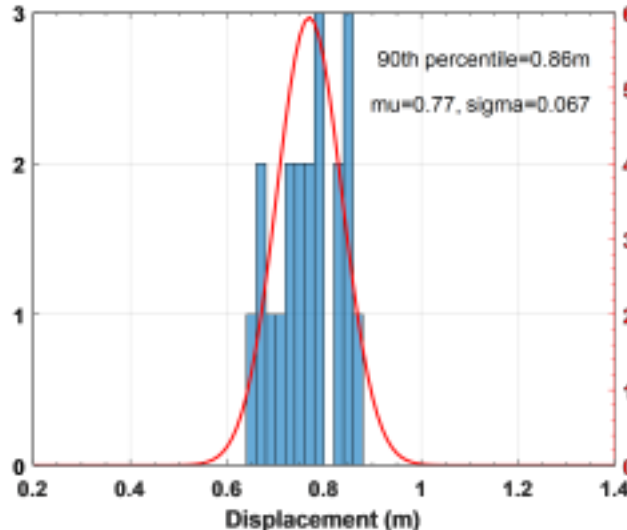


Figure 9. Displacement of the auxiliary building under BDBE ground motion response spectra (GMRS) (PGA = 1.0 g).

As shown in Figure 9, the mean maximum displacement was about 0.77 m. If a normal distribution is assumed, the 90th percentile of the displacement is about 0.86 m (2.81 ft). The superstructure has less than a 10% probability of contact with a hard stop (moat wall) under BDBE GMRS loading, as the codes suggested. In other words, the lower bound of the CS is about 0.86 m in this case.

Upper Bound of CS from UPD

In this research, a fragility curve for the LRBs was estimated from the maximum likelihood method suggested by Shinozuka et al. [2000]. The empirical fragility curve of the LRBs is assumed as a cumulative distribution function of the lognormal distribution, as shown in Equation (1),

$$F(e) = \Phi\left[\frac{\ln(e/e_m)}{\beta_c}\right] \quad (1)$$

where e and e_m are the shear strain (%) and the median value of the strain, respectively, β_c is the log-standard deviation, and $\Phi[\cdot]$ is the cumulative standard normal distribution function.

The likelihood function for the estimation can be defined as Equation (2),

$$L = \prod_{i=1}^N [F(e_i)]^{x_i} [1 - F(e_i)]^{1-x_i} \quad (2)$$

where e_i is the shear strain (%) to which the i th LRB is subjected, $x_i = 1$ or 0 depending on whether the LRB failed or not, and N is the total number of tested LRBs.

Two parameters, e_m and β_c , are estimated from Equation (3), which finds the parameters to maximize the likelihood function L .

$$\frac{d \ln L}{d e_m} = \frac{d \ln L}{d \beta_c} = 0 \quad (3)$$

The median shear failure strain and log-standard deviations were about 413% and 0.051, respectively. Figure 18 shows the empirical fragility curve. The test results in Figure 16 with the highest axial load (Test #6) was not included in this failure probability estimation because it exceeded the range of interest.

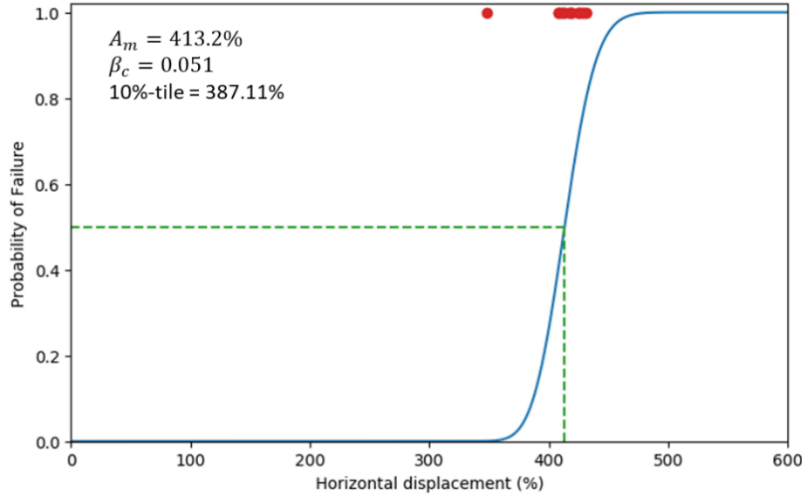


Figure 10. Probability of shear failure.

The failure probability of a prototype LRB in an isolated NPP is assumed to be the same as the small-scale LRBs despite size effects, considering the practical difficulty to conduct ultimate property tests of prototype LRBs. This assumption is considered to be acceptable based on the fact that the shear failure of the full-scale LRB specimen occurred at approximately 515% shear strain level [Kim, J., et al, 2019]. From the fragility curve, the 10th percentile of the failure strain is about 387% or 0.87 m for a full-scale LRB with 0.224 m rubber thickness. Thus, 0.87 m can be the upper bound of the CS to satisfy the performance criteria that the isolation system should have 90% confidence of surviving without loss of gravity-load capacity.

CONCLUSION

In this paper, we integrated NPP and LRB structural models to investigate the response, capacity, and clearance to the stop of an isolated NPP based on given performance criteria. From the experimental results and analysis, the following conclusions are drawn.

- (1). If a normal distribution is assumed for the analysis results of the maximum displacement under BDBE GMRS loading, the 90th percentile of the displacement was about 0.86 m. In this case, CS should be greater than 0.86 m based on the performance criteria that the superstructure has less than a 10% probability of contact with a hard stop (moat wall) under BDBE GMRS loading.
- (2). The shear strain of the LRB can be failure criteria within a certain level of vertical loading based on the UPD, which represents the results of bearing capacity experiments. Failure probability using the shear strain parameter can be calculated by maximum likelihood estimation. The median failure strain was about 413%, and the 10th percentile was about 387% from the estimation. The 387% shear strain means 0.87 m for a full-scale LRB, which can be the upper bound of the CS to satisfy the performance criteria that the isolation system should have 90% confidence of surviving without loss of gravity-load capacity.

Acknowledgments

This work was supported by a National Research Foundation of Korea (NRF) grant funded by the Korean government (NRF-2017M2A8A4014829).

REFERENCES

- ASCE. Seismic Analysis of Safety-Related Nuclear Structures, ASCE/SEI Standard 4-16; ASCE: Reston, VA, USA, 2017.
- Kim, J.; Kim, M.; Choi, I. Experimental study on seismic behavior of lead-rubber bearing considering bi-directional horizontal input motions. *Eng. Struct.* 2019, 198, 109529.
- Kim, M.; Hahm, D.; Kim, J. Development of probabilistic seismic risk assessment methodology for seismically isolated nuclear power plants. In Transactions, SMiRT-25; Charlotte, NC, USA, 2019.
- Kim, M.; Kim, J.; Choi, I. Investigation of Performance Objectives for Seismic Isolation Systems of Nuclear Power Plants, KAERI/TR-4667; 2012.
- Kim, M.; Kim, J.; Hahm, D.; Park, J.; Choi, I. Seismic performance assessment of seismic isolation systems for nuclear power plants, PVP2016-63742 (Presentation only). In Proceedings of the ASME 2016 Pressure Vessels and Piping Conference PVP2016, Vancouver, BC, Canada, 17–21 July 2016.
- Kumar, M.; Whittaker, A.S. On the calculation of the clearance to the hard stop for seismically isolated nuclear power plants. In Transactions, SMiRT-23; Manchester, UK, 2015.
- Mosqueda, G.; Marquez, J.; Hughes, P. Modeling of base-isolated nuclear power plants subjected to beyond design basis shaking. In Proceedings of the 25th Conference on Structural Mechanics in Reactor Technology, Charlotte, NC, USA, 2019.
- OpenSees. Available online: <http://opensees.berkeley.edu> (accessed on).
- Sarebanha, A.; Mosqueda, G.; Kim, M.; Kim, J. Seismic response of base isolated nuclear power plants considering impact to moat walls. *Nucl. Eng. Des.* 2018, 328, 58–72.
- Schellenberg, A.; Baker, J.; Mahin, S.; Sitar, N. Investigation of Seismic Isolation Technology Applied to the APR 1400 Nuclear Power Plant; 2014.
- Schellenberg, A.H.; Sarebanha, A.; Schoettler, M.J.; Mosqueda, G.; Benzoni, G.; Mahin, S.A. Hybrid Simulation of Seismic Isolation Systems Applied to an APR-1400 Nuclear Power Plant; Pacific Earthquake Engineering Research Center: Berkeley, CA, USA, 2015.
- Shinozuka, M.; Feng, M.; Lee, J.; Naganuma, T. Statistical Analysis of Fragility Curves. *J. Eng. Mech.* 2000, 126, 1224–1231.
- U.S.NRC. Technical Considerations for Seismic Isolation of Nuclear Facilities; NUREG/CR-7253; 2019.